On the averaging in the mMulti-Blade Coordinate transformations for wind turbines An H_∞-model matching approach

Mulders, Sebastiaan Paul; Van Wingerden, Jan Willem

DOI
10.1109/CCTA.2018.8511417

Publication date
2018

Document Version
Final published version

Published in
2018 IEEE Conference on Control Technology and Applications (CCTA 2018)

2018 IEEE Conference on Control Technology and Applications (CCTA)
Copenhagen, Denmark, August 21-24, 2018

On the averaging in the Multi-blade Coordinate transformations for wind turbines: an $\mathcal{H}_\infty$ model matching approach

Sebastiaan Paul Mulders[1] and Jan-Willem van Wingerden[1]

***Abstract*— The blade dynamics of a wind turbine are periodic with the angular position of the rotor. For analysis of these dynamics it is common practice to use the so-called Multi-Blade Coordinate (MBC) transformation in combination with a system matrix averaging technique to obtain a linear time-invariant model. The MBC transformation eliminates the periodicity over a rotation of the rotor, while retaining important blade dynamics. However, in the averaging step the inevitable residual periodic dynamics can result in an inaccurate linear representation. This paper shows the inaccuracy of the state-of-the-art averaging technique using a high fidelity two-bladed wind turbine model. The state-of-the-art technique is compared to two novel averaging methods. Results show a close resemblance of the computed models from the proposed methods to the frequency response average, whereas the conventional method shows erroneous results.**

I. INTRODUCTION

The dynamics of individual wind turbine rotor blades are generally described and measured in a rotating frame of reference, and are periodic with the angular position of the rotor (azimuth angle). High-fidelity wind turbine simulation software packages often include options to obtain periodic linearizations including degrees of freedom in a rotating reference frame [1]. Using these periodic models for analysis purposes, one might simply evaluate the mean of all frequency responses over a complete rotation. However, by doing so for periodic systems eliminates dynamics which are often of interest [2]. For this reason, the analysis of wind turbine rotating degrees of freedom for three- and two-bladed turbines is first subject to an Multi-Blade Coordinate (MBC) transformation, eliminating non-essential periodicity over a rotation of the rotor, while retaining the important blade dynamics.

The MBC transformation is used to transform blade load signals and pitch angles from a rotating to a non-rotating reference frame [2]. The main reasoning to do so is to obtain decoupled signals, such that control design for Individual Pitch Control (IPC) is simplified. Transformations like MBC are also used in other fields such as in electrical engineering where it is called direct-quadrature-zero (dq0) transformation to rotate the reference frame of three-phase electrical systems in an effort to simplify the analysis of such systems [3], but also in helicopter theory where it is often referred to as the Coleman transformation [4].

As the main interest of wind turbine design has in the past particularly been focused on three-bladed onshore turbines,

[1]Delft Center for Systems and Control, Faculty of Mechanical Engineering, Delft University of Technology, Mekelweg 2, 2628 CD Delft, The Netherlands. Correspondence to: s.p.mulders@tudelft.nl

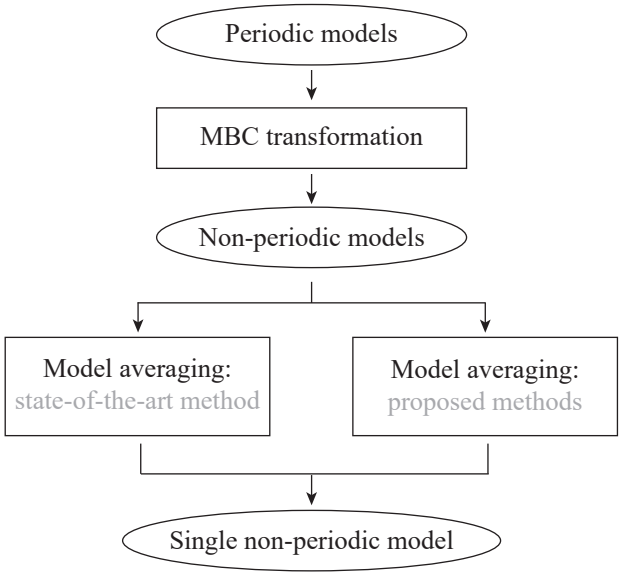

Fig. 1: Periodic linear models are transformed by the Multi-Blade Coordinate transformation to obtain non-periodic system descriptions in the non-rotating coordinate system. Averaging methods of these non-rotating systems is of interest to obtain a single non-periodic model.

MBC transformations for three-bladed turbines are a proven strategy to reduce fatigue loading on wind turbines with individual pitch control capabilities [5]. When applying the MBC transformation of a three-bladed wind turbine in a similar way to a two-bladed turbine, the transformation becomes singular and is not uniquely defined [6]. However, various papers do implement the three-bladed MBC transformation on two-bladed turbines, and show positive results in terms of blade load fatigue reductions [5][7][8].

In the ideal case, application of the MBC transformation to periodic linearizations represent non-periodic Linear Time-Invariant (LTI) systems, independent of the azimuth position. However, in more realistic scenarios using linearized models from non-linear wind turbine simulation software such as FAST, HAWC2 or Bladed, the decoupling is often still weakly-periodic. Now, to obtain a single LTI representation of the transformed models, model averaging techniques are applied. Generally, a matrix averaging method is applied to the A, B, C and D-matrices of the state-space system [9], which in certain cases results in erroneous averages.

In this paper it is confirmed that this matrix averaging procedure can lead to undesirable models and two alternative

978-1-5386-7698-1/18/$31.00 ©2018 IEEE

techniques that outperform the state-of-the-art method are proposed. All methods are applied to the non- or weakly-periodic models after the MBC transformation as shown in Fig. 1. The first proposed method involves augmentation of linear models, followed by a model-order reduction step. The second technique is a model matching technique based on the $\mathcal{H}_\infty$ framework, and combines the obtained periodic linear models in a generalized plant description [10]. This plant is subsequently used to synthesize a $\mathcal{H}_\infty$ optimal model average that minimizes the infinity norm.

The organization of this paper is as follows. First, in Section II, the MBC transformation is introduced and applied to a two-bladed wind turbine. Also, the state-of-the-art state-space averaging technique is described. Next, in Section III, two new model averaging methods are proposed and a benchmark case is defined. In Section IV, the methodologies are applied to MBC transformed linear models obtained from a modified two-bladed version of the NREL5MW reference wind turbine model. Finally, conclusions are drawn in Section V.

II. PROBLEM DESCRIPTION

In this section the general framework of the MBC transformation is explained in Section II-A, followed by a description of the application to a two-bladed rotor configuration in Section II-B. Finally, the state-of-the-art model averaging method, applied to the obtained system is discussed in Section II-C.

A. The Multi-Blade Coordinate transformation

The MBC relations transforming the rotating out-of-plane blade moments M_b^*, to their respective non-rotating degrees of freedom [2] are defined as the forward transformation by

$$M_0 = \frac{1}{B}\sum_{b=1}^{B} M_b^*, \tag{1}$$

$$M_{n\mathrm{c}} = \frac{2}{B}\sum_{b=1}^{B} M_b^* \cos\left(n\psi_b\right), \tag{2}$$

$$M_{n\mathrm{s}} = \frac{2}{B}\sum_{b=1}^{B} M_b^* \sin\left(n\psi_b\right), \tag{3}$$

$$M_{B/2} = \frac{1}{B}\sum_{b=1}^{B} M_b^* (-1)^b, \tag{4}$$

where n is the harmonic number, B the total number of blades, and ψ_b is the azimuth position of blade b with respect to the reference azimuth ψ given by

$$\psi_b = \psi + (b-1)\frac{2\pi}{B}. \tag{5}$$

All degrees of freedom in the rotating frame are denoted as $(\cdot)^*$. The rotor azimuth coordinate system is defined as $\psi = \psi_1 = 0$ when the first blade is in the upright vertical position.

The new non-rotating (fixed) degrees of freedom are called rotor coordinates because they represent the cumulative behavior of all rotor blades. The physical interpretation of the rotor coordinates depends on the degree of freedom it refers to. For example, when M_b^* refers to the out-of-plane flapping moment of the blades, then M_0 is the rotor coning, $M_{1\mathrm{c}}$ is the rotor fore-aft tilt (rotation that is horizontal and normal to the rotor shaft) and $M_{1\mathrm{s}}$ is the rotor side-side coning (rotation that is vertical and normal to the rotor shaft) [2]. The collective and cyclic modes M_0, $M_{1\mathrm{c}}$ and $M_{1\mathrm{s}}$ are most important because of their fundamental role in the coupled motion of the rotor in the non-rotating system. For axial wind flows the collective and cyclic modes of the rotor degrees of freedom couple with the fixed system. The rotor modes corresponding to $M_{n\mathrm{c}}$ $(n > 1)$, $M_{n\mathrm{s}}$ $(n > 1)$ and $M_{B/2}$ are called reactionless modes because they do not cause any load transfer from the rotor to the hub in the fixed frame reference system and correspond purely to internal rotor motion. The mode $M_{B/2}$ is called the differential mode and is only considered for rotors with an equal number of blades.

The inverse transformation that converts the non-rotating frame back to the rotating frame is given by the generalized relation

$$M_b^* = M_0 + \sum_n \left(M_{n\mathrm{c}} \cos\left(n\psi_b\right) + \; M_{n\mathrm{s}} \sin\left(n\psi_b\right)\right) + M_{B/2}(-1)^b. \tag{6}$$

The next section will elaborate on the implementation of the described transformation on a two-bladed wind turbine.

B. Application to a two-bladed wind turbine

Application of the conventional transformation applied to three-bladed turbines, decoupling the blade moments into a rotor tilt and yaw axis, results in a singular transformation [4][6] when applied to a two-bladed case. Therefore, in this section, the implementation and application of the relations defined by (1) and (4) is elaborated. These two equations ($n_{\mathrm{eq}} = 2$), decouple the individual blade loads into a collective and differential mode for a two-bladed wind turbine ($B = 2$), shown in Fig. 2. A description for implementation of the transformation on linear models from a three-bladed wind turbine is given in [2]. This section outlines the most notable implementation differences for application to a two-bladed case.

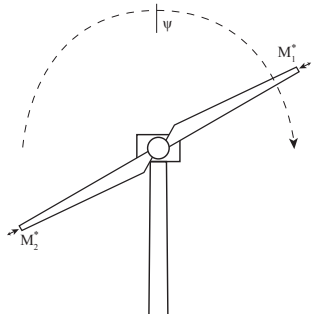

Fig. 2: Schematic presentation of a two-bladed wind turbine showing the rotor azimuth ψ and the out-of-plane blade-root bending moments M_i^* (adapted from [11]).

The dynamics from individual blade pitch angles to blade root out-of-plane bending moments are assumed to be described as second-order systems. This is in accordance with linear systems obtained from the high-fidelity wind turbine simulation software package FAST (Fatigue, Aerodynamics, Structures, and Turbulence) [1]. According to the conditions given in the introduction of this section, the reverse transformation is defined as

$$\begin{bmatrix} M_1^* \\ M_2^* \end{bmatrix} = \tilde{t} \begin{bmatrix} M_0 \\ M_1 \end{bmatrix}, \tag{7}$$

where the reverse transformation matrix $\tilde{t} \in \mathbb{R}^{B \times n_{\mathrm{eq}}}$ is given by

$$\tilde{t} = \begin{bmatrix} 1 & -1 \\ 1 & 1 \end{bmatrix}. \tag{8}$$

The rotating system is related to the non-rotating system by

$$X = T X_{\mathrm{NR}}, \tag{9}$$

where

$$T = \begin{bmatrix} I_{F \times F} & 0 \\ 0 & t \end{bmatrix}, \tag{10}$$

where F represents the amount of fixed-frame degrees of freedom and $t \in \mathbb{R}^{Bm \times n_{\mathrm{eq}} m}$ is a diagonal matrix consisting of $\tilde{t}$, where m is the amount of rotating degrees of freedom.

As it is assumed that the rotating linearized models only include in- and outputs corresponding to rotating degrees of freedom, results in matrices T_{c} and T_{o} being equal to t. For obtaining the forward transformation matrix, the inverse matrices T^{-1}, T_{c}^{-1} and T_{o}^{-1} are required. The forward transformation, transforming the rotating into a non-rotating system, is given by

$$\tilde{t}^{-1} = \begin{bmatrix} 1/2 & 1/2 \\ -1/2 & 1/2 \end{bmatrix}. \tag{11}$$

Now, combining the results, the following relations transform the periodic matrices to a non-rotating reference frame by applying a state-coordinate change

$$A = \begin{bmatrix} T^{-1} & 0 \\ 0 & T^{-1} \end{bmatrix} A^*(\psi) \begin{bmatrix} T & 0 \\ 0 & T \end{bmatrix}, \tag{12}$$

$$B = \begin{bmatrix} T^{-1} & 0 \\ 0 & T^{-1} \end{bmatrix} B^*(\psi) T_{\mathrm{c}}, \tag{13}$$

$$C = T_o^{-1} \begin{bmatrix} C_1^*(\psi) T & C_2^*(\psi) T \end{bmatrix}, \tag{14}$$

$$D = T_o^{-1} D^*(\psi) T_c, \tag{15}$$

where $A^* \in \mathbb{R}^{r \times r}$ and $C^* \in \mathbb{R}^{q \times r}$ are partitioned as

$$A^*(\psi) = \begin{bmatrix} 0 & I \\ A_{\mathrm{K}}^*(\psi) & A_{\mathrm{C}}^*(\psi) \end{bmatrix}, \tag{16}$$

$$C^*(\psi) = \begin{bmatrix} C_1^*(\psi) & C_2^*(\psi) \end{bmatrix}. \tag{17}$$

Generally, a simple matrix-averaging method described in Section II-C suffices to obtain a single LTI representation in the non-rotating frame. However, when the transformed matrices are still weakly-periodic; or when the systems have the same dynamics but the system representations are similar up to a similarity transformation, the matrix-averaging method may yield erroneous results. This statement is true for both three- and two-bladed cases. An illustrative example for a two-bladed wind turbine will be given in the results section of this paper.

C. State-of-the-art model averaging

In this section, the generally applied state-space model averaging technique is described. This method is for instance used in [2], averaging the obtained non-rotating system matrices defined in (12)-(15).

In general, the obtained models after transformation are defined as continuous-time state-space systems of the form

$$G_i = \begin{cases} \dot{x} = A_i x + B_i u \\ y = C_i x + D_i u, \end{cases} \tag{18}$$

where $A \in \mathbb{R}^{r \times r}$, $B \in \mathbb{R}^{r \times p}$, $C \in \mathbb{R}^{q \times r}$ and $D \in \mathbb{R}^{q \times p}$ represent the system state, input, output and direct feed-through matrices, respectively. The state and input vectors are defined by x and u. The subscript $(\cdot)_i$ indicates the i-th state-space system of G. The average state-space model representation is computed as

$$\bar{A} = \frac{1}{N} \sum_{i=1}^{N} A_i, \quad \bar{B} = \frac{1}{N} \sum_{i=1}^{N} B_i, \tag{19}$$

$$\bar{C} = \frac{1}{N} \sum_{i=1}^{N} C_i, \quad \bar{D} = \frac{1}{N} \sum_{i=1}^{N} D_i, \tag{20}$$

where N represents the amount of models in a complete period, and the indication $\bar{(\cdot)}$ indicates the matrix average. All matrix dimensions remain unchanged with respect to the original matrices. Also, the physical meaning of the states is preserved. However, it is yet unclear whether the averaging method leads to the representation resulting in the optimal average, which will be defined as a benchmark case in Section III-A.

The presented averaging method will be referred to as the *sum-averaging method* in the remainder of this paper, and is regarded as the baseline case to the other proposed state-space averaging methods.

III. METHODOLOGY

This section elaborates on the proposed methodologies for state-space system averaging. For this, first a benchmark case is defined in Section III-A to which the considered averaging methods described in Sections III-B and III-C will be evaluated.

A. Benchmark case

For comparison of the described *sum-averaging method* with the proposed averaging methods, the optimal average is defined as the mean of all MBC transformed model

frequency responses on a specified frequency range

$$|G^*(j\omega)| = \frac{1}{N}\sum_{i=1}^{N}|G_i(j\omega)|\,, \tag{21}$$

$$\angle G^*(j\omega) = \frac{1}{N}\sum_{i=1}^{N}\angle G_i(j\omega), \tag{22}$$

where $\{\omega \in V \subset \mathbb{R} \mid V = [\omega_{\min},\ \omega_{\max}]\}$. This frequency response average will be regarded as the benchmark case when comparing the different averaging techniques.

B. Model-order reduction method

The first proposed state-space averaging method uses an augmentation followed by a model-order reduction step, and will be referred to as the *model-order reduction method*. All state-space system matrices in G_i are defined in a new augmented representation as

$$\tilde{A} = \begin{bmatrix} A_1 & 0 & \dots & 0 \\ 0 & \ddots & & \vdots \\ \vdots & & A_{N-1} & 0 \\ 0 & \dots & 0 & A_N \end{bmatrix}, \quad \tilde{B} = \begin{bmatrix} B_1 \\ \vdots \\ B_{N-1} \\ B_N \end{bmatrix}, \tag{23}$$

$$\tilde{C} = \frac{1}{N}\begin{bmatrix} C_1 & \dots & C_{N-1} & C_N \end{bmatrix}, \quad \tilde{D} = \bar{D},$$

denoted by the $\tilde{(\cdot)}$-indication. The matrix dimensions change using this method to $\tilde{A} \in \mathbb{R}^{rN\times rN}$, $\tilde{B} \in \mathbb{R}^{rN\times p}$, $\tilde{C} \in \mathbb{R}^{q\times rN}$ and $\tilde{D} \in \mathbb{R}^{q\times p}$. For consistent evaluation of the proposed method, a model-order reduction step is included to obtain a model average system with the same dimensions as the original system. The subsequent steps imply that the physical state meaning of the original system is lost.

The order reduction technique consists out of two consecutive operations. First a Hankel Singular Value (HSV) analysis of the considered system is performed, which shows the input-to-state and state-to-output energy transfers [12]. Hankel singular values are often used for model-order estimation and reduction, such that small Hankel singular values signal states are discarded to simplify the model [13]. Then, this information is used to derive a reduced-order state-space approximation by a numerical robust order-reduction method that circumvents the need for ill-conditioned projection matrices [14].

C. $\mathcal{H}_\infty$ model matching method

This section provides a framework incorporating the linear transformed models in a generalized plant P, and synthesizes a model average by $\mathcal{H}_\infty$-synthesis. The structure of P is presented in Fig. 3. All transformed models G_i are gathered in a feed-forward generalized plant set-up, where the input signal w is supplied to all models. The output y of the generalized plant is equal to input w and is fed to the computed model average output, which produces the input u. This signal is subtracted from the distinct linear model outputs. In this way, the model error residuals $z_i = y_i - u$ are

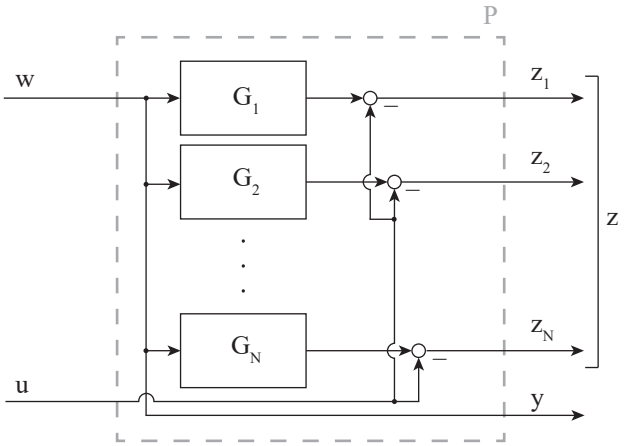

Fig. 3: The transformed linear models are included in generalized plant P, and the output z consists of the error between the output of G_i and an input u. The feed-forward excitation signal w is fed to each linear model G_i and is also available as a direct feed-through output signal y.

computed, which are collected in the performance channel z. The resulting structure of the generalized plant is

$$\begin{bmatrix} z \\ y \end{bmatrix} = \left[\begin{array}{c|c} \hat{G} & -1 \\ \hline 1 & 0 \end{array}\right] \begin{bmatrix} w \\ u \end{bmatrix} = P \begin{bmatrix} w \\ u \end{bmatrix} \tag{24}$$

where $\hat{G} = [G_1,\ G_2 \dots G_N]^T$. The resulting state-space matrices of P are defined as

$$\hat{A} = \tilde{A}, \quad \hat{B} = \begin{bmatrix} \tilde{B},\ 0 \end{bmatrix}, \quad \hat{C} = \begin{bmatrix} \mathrm{diag}(C_1, C_2 \dots C_N) \\ \mathbf{0} \end{bmatrix},$$

$$\hat{D} = \left[\begin{array}{c|c} \mathrm{vec}(D_1, D_2 \dots D_N) & -\mathbf{1} \\ \hline 1 & 0 \end{array}\right], \tag{25}$$

where the state-space matrices (and thus P) are of the same order as the augmented system in (23). The main goal of the $\mathcal{H}_\infty$ model matching technique is to find an average model over a set of transformed linear models. As the methodology is implemented in a feed-forward manner, a necessary condition is that all models are open-loop stable, i.e., all real parts of the eigenvalues of the state A-matrix are negative.

The approach implementation is presented in Fig. 4. The frequency range is bounded by putting a performance weight on the output channel z in the form of a band-pass filter, which is defined as a combination of a second-order low- and high-pass filter

$$\begin{aligned} \Pi(s, \omega_{\min}, \omega_{\max}) &= \mathcal{L}(s, \omega_{\max})\mathcal{H}(s, \omega_{\min}) \\ &= \frac{\omega_{\max}^2}{s^2 + 2\zeta\omega_{\max}s + \omega_{\max}^2}\frac{s^2}{s^2 + 2\zeta\omega_{\min}s + \omega_{\min}^2}, \end{aligned} \tag{26}$$

where the former mentioned filter limits the performance upper bound frequency $\omega_{\max}$, and the latter mentioned the lower bound $\omega_{\min}$.

After synthesis, the model average K_{U} has the same order as P, and produces an output u such that the infinity-norm

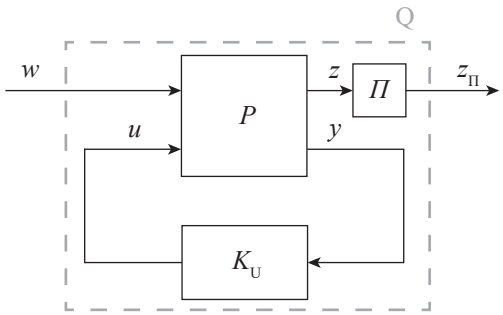

Fig. 4: The transformed linear models are incorporated in generalized plant P, and K_{U} is the best model average minimizing the infinity-norm of Q. The output z_{Π} consists of weighted model output error residual signals.

of

$$||Q(s)||_{\infty} := \sup_{\omega \in V} \sigma_{\max}\left[Q(j\omega)\right], \tag{27}$$

is minimized, and Q is the linear fractional transformation (LFT)

$$Q = \Pi P_{11} + \Pi P_{12} K_{\mathrm{U}} (I - P_{22} K_{\mathrm{U}})^{-1} P_{21}. \tag{28}$$

The main difference between the described and the model-order reduction method is that the generalized plant setting does not yet perform matrix averaging for the C and D matrices, as is concluded by comparing $\tilde{C}$ with $\hat{C}$, and $\tilde{D}$ with $\hat{D}$. This leaves more freedom for arriving at the actual model average during the model synthesis procedure. Another important advantage of the $\mathcal{H}_{\infty}$ framework is the ability to include weighting on a frequency range of interest.

However, a disadvantage of the $\mathcal{H}_{\infty}$ method is that all models included in P need to be stable, whereas for the reduction method unstable models are only troublesome during the order-reduction step – but this step can be disregarded in such cases. The time efficiency of the $\mathcal{H}_{\infty}$ method is highly dependent on the order of the generalized plant P. Also, both methods give average model representations in which the state vectors have no physical meaning.

IV. RESULTS: AVERAGING OF TWO-BLADED NON-ROTATING MATRICES

This section shows the results of the proposed model averaging techniques, and compares them to the conventional averaging method. First, in Section IV-A, the example case is defined which will be used in Section IV-B to evaluate the performance of the different techniques.

A. Case description: load decoupling of a two-bladed rotor

In the wind turbine community, the National Renewable Energy Laboratory (NREL) offshore 5-MW (NREL5MW) baseline wind turbine is a fictive but fully defined reference wind turbine model, which is actively used in the scientific field [15]. The example case that is taken in this paper consists of a modified version of the NREL5MW turbine: one blade is removed such that a two-bladed version of the

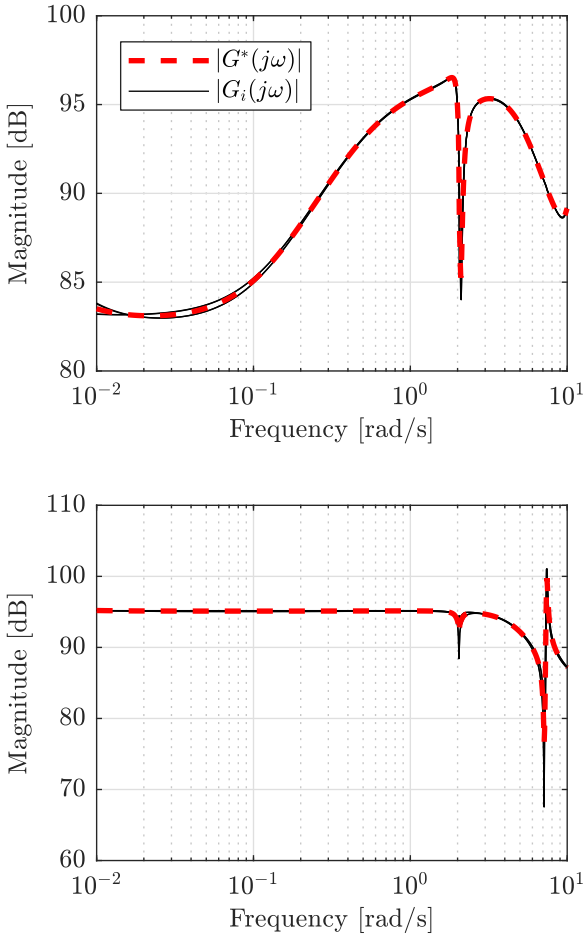

Fig. 5: Bode magnitude plots of the collective and differential moments M_0 (upper) and M_1 (lower) of a two-bladed wind turbine. The responses are still weakly periodic and their frequency response average is given by the red dashed line.

turbine is obtained. This is done using the `FASTv8GUI` [16], which is a `MATLAB`-based Graphical User Interface (GUI) providing convenient interaction with NREL's FAST v8.16. Only a single blade is removed from the model, and all remaining structural properties of the reference wind turbine remain unchanged.

Using the two-bladed model together with the wind turbine simulation software package FAST, periodic models are obtained by linearizing at a fixed rotor and wind speed of 11.98 rpm and 25 m/s, respectively. For linearization purposes, corresponding fixed pitch angle and generator torque settings are used for stable open-loop above-rated operation.

As shown in Fig. 2, the rotor angular position is defined as the azimuth angle ψ and the blade-root moment as M_i^*. Linearization is performed at 4 distinct and evenly spaced azimuth angles over a single rotation. The obtained periodic linear models are subsequently post-processed using the two-bladed linear transformation as described in Section II-B. The resulting Bode plots of the diagonal terms, showing the decoupling in a collective and differential mode are presented in Fig. 5. It is shown that the responses are still weakly

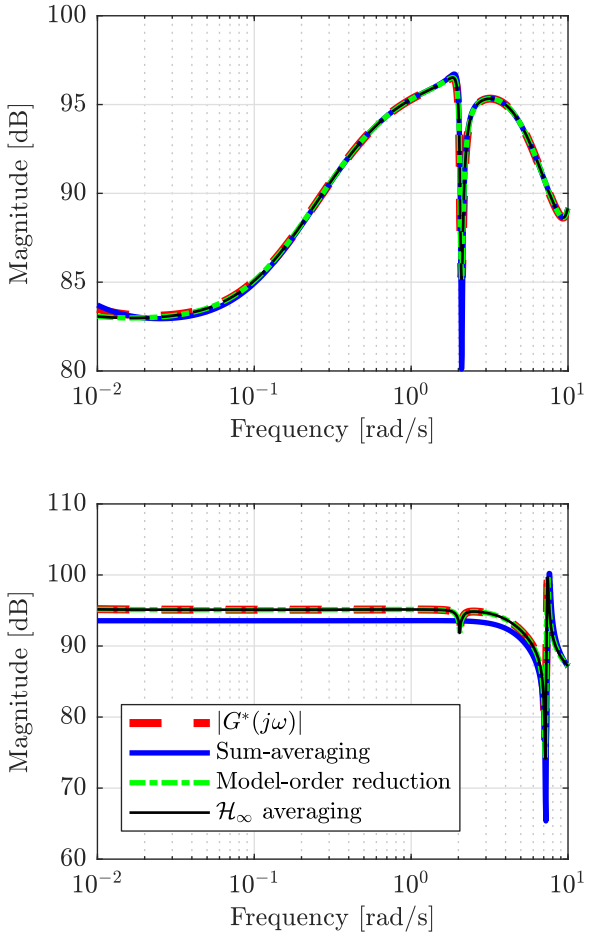

Fig. 6: Average Bode magnitude plots of the collective and differential moments M_0 (upper) and M_1 (lower), using the different averaging techniques. In the collective mode, the resonance attains a significant lower value for the sum-averaging method compared to the other methods. In the collective mode, a clear bias in the low-frequency range is shown, as well as the disappearance of a resonance peak and a frequency peak shift.

periodic, and the frequency response averages are presented in the same figures. The averages serve as a benchmark case for the different averaging methods. For this reason, the averaged responses will only be shown in the subsequent plots.

B. Evaluation of averaging methods

In this section the proposed model averaging techniques are evaluated and compared to the sum-averaging technique. The performance is evaluated by comparing to the obtained average frequency responses shown in Fig. 5.

The sum-averaging method shows, for both the differential and collective mode, a clear deviation from the benchmark case in Fig. 6. For the collective mode, the peak magnitude is larger than the frequency response average. For the differential mode, a clear offset is seen at lower frequencies, while also the resonance peak completely disappears at higher

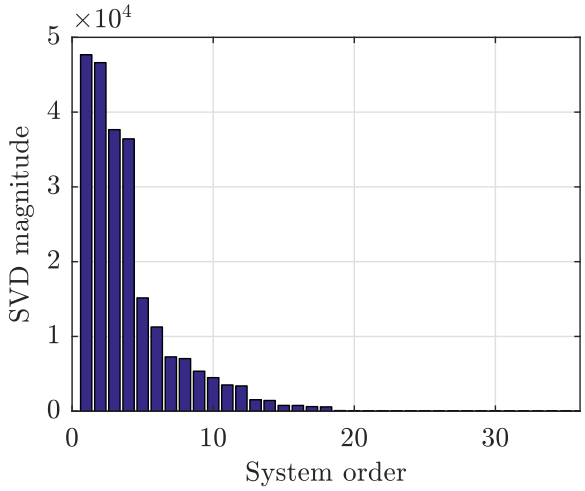

Fig. 7: Hankel singular values of the augmented dynamic system $\tilde{G}$ for the collective mode, showing that the amount of significant augmented system SVD magnitudes is lower than the order of a single system G_i.

frequencies. A slight shift is seen at the location of the last resonance peak. This erroneous result is caused by the averaging of systems with similar dynamics, but subject to a state-coordinate change. Averaging the state-space matrices of such systems possibly results in erroneous outcomes as seen in this example.

The model-order reduction averaging technique shows a close resemblance to the benchmark case. By evaluating the Hankel singular values of the augmented dynamic system in Fig. 7, it is shown that the amount of significant augmented system SVD magnitudes is lower than the order of a single system G_i, which justifies the use of model-order reduction. The HSV information is subsequently used for performing the actual order-reduction step.

The $\mathcal{H}_\infty$ averaging method shows a similar result as the previous described method, following the trajectory of the benchmark response closely. The output performance weight $\Pi(s)$ is defined in the interval $\omega_{\min} = 10^{-2}$ to $\omega_{\max} = 10^1$ rad/s, with a damping of $\zeta = 1/\sqrt{2}$.

A qualitative comparison of the three considered methods is presented in Table I. The sum-averaging method is the simplest to implement as it only consists of element-wise matrix operations. For the proposed methods, more in-depth knowledge is required for set-up and configuration, but coin-

TABLE I: Properties and advantages/disadvantages of the averaging methods

	Averaging	*Order red.*	$\mathcal{H}_\infty$
Ease of implementation	++	+	+/-
Frequency weighting	No	No	Yes
Model order unchanged	Yes	Possibly	Possibly
Stable models needed	No	Partially	Yes
Physical state meaning	Yes	No	No
Accuracy	–	+	++
Time efficiency	++	+	Order dep.

cidently gives more freedom in terms of frequency weighting and model-order selection. Open-loop model stability is not necessary for the state-of-the-art and augmentation step in the model-order reduction method. However. for the order-reduction step and $\mathcal{H}_\infty$ method, open-loop stability is required. For both proposed methods, the state vectors lose their physical interpretations, whereas their accuracy is superior in terms of minimizing the error to the true average frequency response. The time efficiency for the $\mathcal{H}_\infty$ method is highly dependent on the order of the generalized plant P. Application of one of the averaging methods is clearly a trade-off between the described aspects.

V. CONCLUSIONS

Performing a transformation to azimuth dependent linearizations of the established two-bladed NREL5MW model, yields system representations in which the periodicity is largely reduced, resulting in LTI descriptions over all azimuth angles. However, all transformed matrices are similar up to a similarity transformation. Summing and averaging the system matrices may in this case lead to an erroneous description compared to the true average frequency response of the transformed systems. Two averaging methods, based on system augmentation followed by a model-order reduction step, and a method using the $\mathcal{H}_\infty$ framework are proposed. Both methods show a close match to the magnitude frequency response of the benchmark case, outperforming the results obtained from the state-of-the-art averaging method.

REFERENCES

[1] NWTC OpenFAST http://openfast.readthedocs.io [Online; accessed 14-November-2017]

[2] G. Bir, Multi-blade coordinate transformation and its application to wind turbine analysis. 46th AIAA aerospace sciences meeting and exhibit. 2008.

[3] R.H. Park, Two Reaction Theory of Synchronous Machines. AIEE Transactions 48:716-730 (1929).

[4] W. Johnson, Helicopter theory. Courier Corporation, 2012.

[5] E.A. Bossanyi, P.A. Fleming and A.D. Wright. Validation of individual pitch control by field tests on two-and three-bladed wind turbines. IEEE Transactions on Control Systems Technology 21.4 (2013): 1067-1078.

[6] E. van Solingen and J.W. van Wingerden. Linear individual pitch control design for twobladed wind turbines. Wind Energy 18.4 (2015): 677-697.

[7] E.A. Bossanyi and A.D. Wright. "Field testing of individual pitch control on the NREL CART-2 wind turbine." European Wind Energy Conference. 2009.

[8] E.A. Bossanyi, A.D. Wright and P.A. Fleming. Controller field tests on the NREL CART2 turbine. No. NREL/TP-5000-49085. National Renewable Energy Lab.(NREL), Golden, CO (United States), 2010.

[9] G.S. Bir, Users Guide to MBC3: Multi-Blade Coordinate Transformation Code for 3-Bladed Wind Turbines. NREL, 2010

[10] S. Skogestad and I. Postlethwaite, Multivariable feedback control: analysis and design. Vol. 2. New York: Wiley, 2007.

[11] F.D. Bianchi, Wind turbine control systems. Springers, 2007

[12] W. Gawronski and J.-N. Juang, Model reduction in limited time and frequency intervals. International Journal of Systems Science 21.2, 1990: 349-376.

[13] S.-Y. Kung, K.S. Arun and D.V. Bhaskar Rao, State-space and singular-value decomposition-based approximation methods for the harmonic retrieval problem. JOSA 73.12 (1983): 1799-1811.

[14] A. Varga, Balancing free square-root algorithm for computing singular perturbation approximations. Decision and Control, 1991., Proceedings of the 30th IEEE Conference on. IEEE, 1991.

[15] J. Jonkman, S. Butterfield, W. Musial and G. Scott, Definition of a 5-MW reference wind turbine for offshore system development. No. NREL/TP-500-38060. National Renewable Energy Lab (NREL), Golden, CO (United States), 2009.

[16] R. Bos, M. Zaaijer, S.P. Mulders and J.W. van Wingerden: FASTv8GUI, https://github.com/TUDelft-DataDrivenControl/FASTv8GUI, 2018.